Research Article | Vol. 26, No. 18 | 3 Sep 2018 | OPTICS EXPRESS 22615
Optics EXPRESS

# Remote and autonomous temperature measurement based on 3D liquid crystal microlasers

GREGOR PIRNAT,[1] MATJAŽ HUMAR,[1,2] AND IGOR MUŠEVIČ[1,2,*]

[1] *Condensed Matter Department, J. Stefan Institute, Jamova 39, SI-1000 Ljubljana, Slovenia*
[2] *Faculty of Mathematics and Physics, University of Ljubljana, Jadranska 19, SI-1000, Ljubljana, Slovenia*
[*] *igor.musevic@ijs.si*

**Abstract:** We demonstrate non-contact temperature measurement with one tenth of a kelvin precision at distances of several meters using omnidirectional laser emission from dye-doped cholesteric liquid crystal droplets freely floating in a fluid medium. Upon the excitation with a pulsed laser the liquid crystal droplet emits laser light due to 3D Bragg lasing in all directions. The spectral position of the lasing is highly dependent on temperature, which enables remote and contact-less temperature measurement with high precision. Both laser excitation and collection of light emitted by microlasers is performed through a wide telescope aperture optics at a distance of up to several meters. The optical excitation volume, where the droplets are excited and emitting the laser light is of the order of ten cubic millimeters. The measurement is performed with ten second accumulation time, when several droplets pass through the excitation volume due to their motion. The time of measurement could easily be shortened to less than a second by increasing the rate of the excitation laser. Since the method is based solely on measuring the spectral position of a single and strong laser line, it is quite insensitive to scattering, absorption and background signals, such as autofluorescence. This enables a wide use in science and industry, with a detection range exceeding tens of meters.



**OCIS codes:** (120.0280) Remote sensing and sensors; (140.3945) Microcavities; (160.3710) Liquid crystals; (280.3420) Laser sensors; (280.6780) Temperature.

## References and links

1. P. de Gennes and J. Prost, *The physics of liquid crystals* (Oxford University, 1993).
2. H. Coles and S. Morris, "Liquid-crystal lasers," *Nat. Photonics* **4**, 676 (2010).
3. V. I. Kopp, B. Fan, H. Vithana, and A. Z. Genack, "Low-threshold lasing at the edge of a photonic stop band in cholesteric liquid crystals," *Opt. letters* **23**, 1707–1709 (1998).
4. B. Taheri, A. Munoz, P. Palffy-Muhoray, and R. Twieg, "Low threshold lasing in cholesteric liquid crystals," *Mol. Cryst. Liq. Cryst. Sci. Technol. Sect. A. Mol. Cryst. Liq. Cryst.* **358**, 73–82 (2001).
5. E. Alvarez, M. He, A. Munoz, P. Palffy-Muhoray, S. Serak, B. Taheri, and R. Twieg, "Mirrorless lasing and energy transfer in cholesteric liquid crystals doped with laser dyes," *Mol. Cryst. Liq. Cryst. Sci. Technol. Sect. A. Mol. Cryst. Liq. Cryst.* **369**, 75–82 (2001).
6. S. Morris, A. Ford, M. Pivnenko, and H. Coles, "Enhanced emission from liquid-crystal lasers," *J. Appl. Phys.* **97**, 023103 (2005).
7. S. M. Jeong, N. Y. Ha, Y. Takanishi, K. Ishikawa, H. Takezoe, S. Nishimura, and G. Suzaki, "Defect mode lasing from a double-layered dye-doped polymeric cholesteric liquid crystal films with a thin rubbed defect layer," *Appl. physics letters* **90**, 261108 (2007).
8. F. Araoka, K.-C. Shin, Y. Takanishi, K. Ishikawa, H. Takezoe, Z. Zhu, and T. M. Swager, "How doping a cholesteric liquid crystal with polymeric dye improves an order parameter and makes possible low threshold lasing," *J. applied physics* **94**, 279–283 (2003).
9. M. Humar, M. Ravnik, S. Pajk, and I. Muševič, "Electrically tunable liquid crystal optical microresonators," *Nat. Photonics* **3**, 595 (2009).
10. I. Muševic and M. Humar, "Tunable liquid crystal optical microcavities," in *Emerging Liquid Crystal Technologies VI,* vol. 7955 (International Society for Optics and Photonics, 2011), p. 795509.
11. I. Muševič, "Integrated and topological liquid crystal photonics," *Liq. Cryst.* **41**, 418–429 (2014).
12. M. Humar and I. Muševič, "3D microlasers from self-assembled cholesteric liquid-crystal microdroplets," *Opt. express* **18**, 26995–27003 (2010).

#338089 https://doi.org/10.1364/OE.26.022615
Journal © 2018 Received 9 Jul 2018; revised 27 Jul 2018; accepted 28 Jul 2018; published 20 Aug 2018

Optics EXPRESS

13. R. J. Carlton, J. T. Hunter, D. S. Miller, R. Abbasi, P. C. Mushenheim, L. N. Tan, and N. L. Abbott, "Chemical and biological sensing using liquid crystals," *Liq. crystals reviews* **1**, 29–51 (2013).
14. Y.-D. Jung, M. Khan, and S.-Y. Park, "Fabrication of temperature- and pH-sensitive liquid-crystal droplets with PNIPAM-b-LCP and SDS coatings by microfluidics," *J. Mater. Chem. B* **2**, 4922–4928 (2014).
15. M. Humar, "Liquid-crystal-droplet optical microcavities," *Liq. Cryst.* **43**, 1937–1950 (2016).
16. H.-G. Lee, S. Munir, and S.-Y. Park, "Cholesteric liquid crystal droplets for biosensors," *ACS applied materials & interfaces* **8**, 26407–26417 (2016).
17. S. Munir and S.-Y. Park, "Liquid-crystal droplets functionalized with a non-enzymatic moiety for glucose sensing," *Sensors Actuators B: Chem.* **257**, 579–585 (2018).
18. M. Humar and I. Muševič, "Surfactant sensing based on whispering-gallery-mode lasing in liquid-crystal micro-droplets," *Opt. Express* **19**, 19836–19844 (2011).
19. I.-H. Lin, D. S. Miller, P. J. Bertics, C. J. Murphy, J. J. De Pablo, and N. L. Abbott, "Endotoxin-induced structural transformations in liquid crystalline droplets," *Science* **332**, 1297–1300 (2011).
20. T. Bera, J. Deng, and J. Fang, "Protein-induced configuration transitions of polyelectrolyte-modified liquid crystal droplets," *The J. Phys. Chem. B* **118**, 4970–4975 (2014).
21. M. Khan and S.-Y. Park, "Specific detection of avidin–biotin binding using liquid crystal droplets," *Colloids Surfaces B: Biointerfaces* **127**, 241–246 (2015).
22. U. Manna, Y. M. Zayas-Gonzalez, R. J. Carlton, F. Caruso, N. L. Abbott, and D. M. Lynn, "Liquid crystal chemical sensors that cells can wear," *Angewandte Chemie Int. Ed.* **52**, 14011–14015 (2013).
23. P. Childs, J. Greenwood, and C. Long, "Review of temperature measurement," *Rev. scientific instruments* **71**, 2959–2978 (2000).
24. X.-d. Wang, O. S. Wolfbeis, and R. J. Meier, "Luminescent probes and sensors for temperature," *Chem. Soc. Rev.* **42**, 7834–7869 (2013).
25. F. Vetrone, R. Naccache, A. Zamarron, A. Juarranz de la Fuente, F. Sanz-Rodriguez, L. Martinez Maestro, E. Martiin Rodriguez, D. Jaque, J. Garcia Solee, and J. A. Capobianco, "Temperature sensing using fluorescent nanothermometers," *ACS nano* **4**, 3254–3258 (2010).
26. R. Zeltner, R. Pennetta, S. Xie, and P. S. J. Russell, "Flying particle microlaser and temperature sensor in hollow-core photonic crystal fiber," *Opt. letters* **43**, 1479–1482 (2018).
27. E. P. Schartner and T. M. Monro, "Fibre tip sensors for localised temperature sensing based on rare earth-doped glass coatings," *Sensors* **14**, 21693–21701 (2014).
28. M. Humar, A. Dobravec, X. Zhao, and S. H. Yun, "Biomaterial microlasers implantable in the cornea, skin, and blood," *Optica* **4**, 1080–1085 (2017).
29. P. V. Shibaev, R. L. Sanford, D. Chiappetta, and P. Rivera, "Novel color changing pH sensors based on cholesteric polymers," *Mol. Cryst. Liq. Cryst.* **479**, 161–1199 (2007).
30. V. Stroganov, A. Ryabchun, A. Bobrovsky, and V. Shibaev, "A novel type of crown ether-containing metal ions optical sensors based on polymer-stabilized cholesteric liquid crystalline films," *Macromol. rapid communications* **33**, 1875–1881 (2012).
31. S. Kado, Y. Takeshima, Y. Nakahara, and K. Kimura, "Potassium-ion-selective sensing based on selective reflection of cholesteric liquid crystal membranes," *J. Inclusion Phenom. Macrocycl. Chem.* **72**, 227–232 (2012).
32. M. Moirangthem, R. Arts, M. Merkx, and A. P. Schenning, "An optical sensor based on a photonic polymer film to detect calcium in serum," *Adv. Funct. Mater.* **26**, 1154–1160 (2016).
33. P. V. Shibaev, D. Chiappetta, R. L. Sanford, P. Palffy-Muhoray, M. Moreira, W. Cao, and M. M. Green, "Color changing cholesteric polymer films sensitive to amino acids," *Macromolecules* **39**, 3986–3992 (2006).

## 1. Introduction

Liquid crystals (LCs) [1] are orientational ordered fluids that find a variety of display and photonic applications due to their exceptionally high optical birefringence and the ability to respond to weak external fields. Furthermore, liquid crystals show a huge variety of differently ordered phases, which have different optical and structural properties. Among them the chiral phases have attracted a lot of interest for application in liquid crystal lasers [2–8]. Namely, due to molecular chirality, liquid crystals show spontaneous helicoidal ordering, which exhibits a one-dimensional photonic band gap. This band gap can be tuned by chemistry of materials from the UV to the infrared spectrum. Based on their photonic band gap properties, chiral nematic liquid crystals can be used to make tuneable dye lasers, where the fluorescent dye is mixed with a liquid crystal to produce a uniformly distributed optical gain medium within the 1D periodic optical resonator. The advantage of chiral liquid crystal lasers is that they are formed spontaneously, without the need of advanced manufacturing, which is required for solid state optical devices.

Recently there has been an increased interest in making photonic devices of micrometer

Optics EXPRESS

size, such as optical microcavities and microlasers made of liquid crystals. Humar and Muševič et al. [9–11] have demonstrated in a number of papers that excellent photonic microdevices can be made by simply dispersing liquid crystals in another liquid, which is immiscible with the liquid crystal. They have demonstrated operation of tuneable whispering gallery mode (WGM) resonators made of small droplets of a nematic liquid crystal of typically ten micrometer diameter [9]. Omnidirectional lasing has been demonstrated from chiral nematic liquid crystals droplets down to 15 $\mu$m in diameter [12]. In these devices the photonic band gap is spontaneously created by dispersing the liquid crystal in water, glycerol or other immiscible fluid. Due to surface molecular ordering, an onion-like structure of molecules is formed in a fraction of a second throughout the droplet. With fluorescent dye molecules dispersed in the layered structure inside the droplet, a dye microlaser that emits the laser light in all directions is obtained.

Because the orientation of liquid crystal molecules at interfaces is very sensitive to the outside environment, LC droplets and flat films have been used to detect a variety of quantities [13], including temperature [14, 15], electric [9] and magnetic field, pH [14, 16], glucose [16, 17], surfactants [18], endotoxins [19], proteins [20, 21] and biological properties [22]. Even slight change of molecular orientation at the interface produces strong changes throughout the liquid crystal layer. In this way, tiny surface perturbation is strongly amplified in the structure and this causes huge changes in photonic properties. In most cases the readout of this structural change is done under the microscope by observing the LC patterns under crossed polarizers or by measuring the reflectance spectra for cholesteric liquid crystals (CLC) droplets. While these methods work when the flat LC films and droplets are observed under the microscope, they are more difficult to implement for remote sensing at separations of a couple of meters.

We have shown previously that optical read-out can be performed by laser emission of whispering-gallery modes (WGMs) in nematic LC droplets [9, 15, 18]. The eigenfrequencies of the WGMs are extremely sensitive to the changes in the refractive index of the droplet, which makes them a perfect candidate for remote optical read-out. However, the WGMs are also highly dependent on the size of the droplet, which is a serious drawback, because we do not know the size of the droplet in advance to a good-enough precision. In this case only relative changes on a particular droplet can be measured, but as soon as we have a sample of polydispersed droplets this becomes more difficult. There is an elegant solution to this problem by using Bragg lasing from CLC droplet lasers [12] instead of WGM lasing. The position of the Bragg lasing line depends solely on the period of the Bragg structure and not on the size of the droplet. The CLC lasers are readily formed from droplets, which can be used as stand-alone probes, emitting laser light in all directions. The lasing wavelength is usually highly dependent on the temperature due to the intrinsic temperature dependence of the helical period. CLC microdroplets can therefore be used as temperature probes; they can be freely floating in a carrier medium, they are optically pumped at a distance and they flash-back a laser pulse because they are emitting the laser light in all directions. These 3D microlasers are therefore ideal temperature microsensors.

Temperature measurements are extremely important in all areas of industry, research and every day life. The temperature is measured in a contact way or remotely [23]. The most widely used passive remote temperature measurement is using infrared thermometer measuring the black body radiation. Active remote temperature measurements include for example Rayleigh scattering, Raman scattering, spectral reflectometry and luminescent methods. Luminescent methods use luminiscent molecules or nanoparticles, whose optical properties, such as fluorescent intensity and lifetime change with temperature [24]. Both passive and active temperature measurements are usually limited by the thermal and optical properties of the measured objects. Most of these methods rely on the small spectral shifts or relative changes in signal intensities, where the spectral intensity distribution is broad. For example, nanothermometers in a form of fluorescent nanoparticles doped with $Er^{3+}$ dopants have been used to measure the temperature of living cells [25]. Local temperature sensing can also be performed by using rare-earth doped tips

Optics EXPRESS

of optical fibres [26] or using WGM spectrum of a single dye-doped particle inside a hollow fibre [27]. Substances inside the measured sample can significantly distort the signal by absorption and presence of addition signals, such as autofluorescence and Raman peaks. This limits the accuracy especially in inhomogeneous samples.

Here we demonstrate optical excitation and lasing from chiral nematic microdroplets freely floating in glycerol/water solution at a separation of a couple of meters. We show that our method is advantageous, because the 3D microlasers provide strong optical signals propagating in all directions, independent on the orientation of the microlasers. Millions of microlaser sensors can be produced in a fraction of a second and they all emit the laser light at the same wavelength, which is solely determined by the structural period of the CLC material and is independent on their size. The optical read-out signal, emitted by the microlasers is in the form of very narrow spectral peak, whose spectral position is independent upon propagation through absorbing, scattering or fluorescent medium. The production of the CLC droplets is extremely simple and scalable and they can also be made from bio-compatible and nontoxic materials [28], making them useful for monitoring temperature in biological and chemically sensitive systems.

## 2. Experimental section

### 2.1. Optical setup for remote sensing

An optical system was constructed to focus the excitation laser onto the remote sample and to collect the lasing signal from the 3D microlasers, as shown in Figs. 1(a) and 1(b). The optical components were housed inside a commercial astronomical telescope tube to provide a stable optical platform. The nanosecond pulsed pump laser (optical parametric oscillator, Opotek) operated at 532 nm and 20 Hz and the spectrometer (Andor Shamrock, SR-500) were coupled via optical fibers to the optical system inside the telescope tube. The setup was composed of a large 200 mm diameter plan-convex lens with focal length of 400 mm (Edmund Optics). For other optical elements inside the tube, a cage system (Thorlabs) was used to hold them in place in the central axis of the telescope. The elements inside the cage system were longpass 550 nm dichroic mirror (Thorlabs), longpass filter (Thorlabs), 50 mm diameter biconvex lens and 2 fiber collimators (air-spaced doublet, Thorlabs). The position of the small lens was changed by sliding it along the cage rails, thus positioning the focal point of the optical system closer/further away from the telescope. The measurements were performed at the distance of 1-3 meters from the telescope. The pump pulse energy at the focal point was in the range of 100-600 $\mu$J. The pump laser was coupled into the telescope via 550 $\mu$m core diameter multimode optical fiber. The received signal was coupled to the spectrometer with a 105 $\mu$m core diameter multimode fiber.

### 2.2. Preparation of liquid-crystal droplets

A mixture of MLC-7023 ($n_e$=1.53 and $n_\circ$ = 1.46) liquid crystal (Merck), S-811 chiral dopant (Merck) and Pyrromethane 580 fluorescent dye (Exciton) were used to prepare the CLC droplets. The phase transition temperature of pure MLC-7023 into the isotropic phase is 90.0 °C. Two different LC mixtures were made: Sample 1 with 25 wt% of S-811, and Sample 2 with 26 wt% of S-811. The phase transition temperature into the isotropic phase was around 60 °C. For both LC samples approximately 0.2 wt% Pyrromethane dye was used. To dissolve the dye the mixture was heated to above the clearing point, subsequently cooled and centrifuged to remove any solid particles that might have been left in the mixture. The CLC mixture was dispersed in glycerol at room temperature by manually mixing both components. The droplet mixture was inspected with optical microscope to check weather droplets contained defects, which are known to inhibit lasing. If numerous defects in CLC droplets were spotted, the mixture was put on a hot plate at 50 °C for periods of 1 min, while being constantly stirred to prevent droplets from floating to the surface and segregating at the glycerol-air interface. After the droplets of sizes below 100

Optics EXPRESS

microns stabilized, a typical radially symmetric structure was observed. Afterwards, 1 wt% PVA (polyvinyl alcohol) water solution (50-90 % in total volume) was added to decrease the viscosity. This caused the liquid system to be less viscous and easier to stir with a magnetic stirrer; during the experiment, the constant flow prevented droplets from sticking to the glass surface of the container as well as preventing the droplets from segregating at the liquid-air interface. The refractive index of the carrier fluid after adding 1 wt% PVA water solution was less than the refractive index of the CLC mixture, which also enabled WGM lasing in addition to the 3D Bragg lasing.

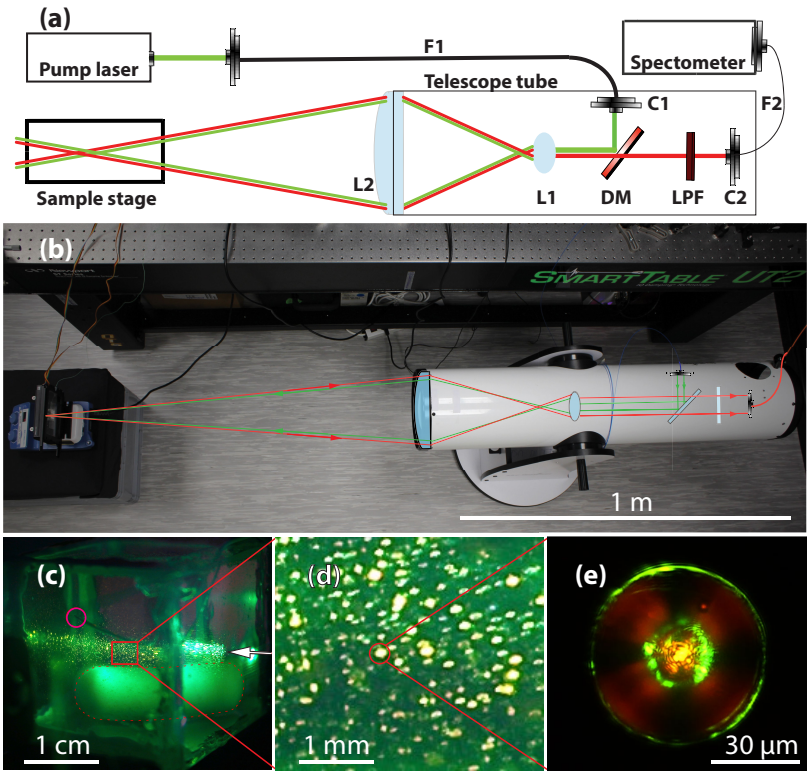


Fig. 1. a) Schematics of the optical setup: Pump laser is a 10 ns, 532 nm laser; F1 - optical fibre of 550 $\mu$m core diameter. Telescope tube is taken from a low cost commercial telescope; DM - longpass dichroic mirror; L1 - 50 mm diameter biconvex lens with focal length of 60 mm; L2 - 200 mm diameter plan-convex focusing lens with focal length of 400 mm; Sample stage with magnetic stirrer and temperature sensor is enclosed into a box with windows; LPF - Longpass 550 nm dichroic filter; F2 - a 105 $\mu$m core diameter fiber; Andor Shamrock SR-500 spectrometer. b) Picture of the optical setup with beam paths superimposed. c) Picture of the sample. CLC droplets were dispersed in a mixture of gycerol and water inside a glass container (25 mm $\times$ 24 mm $\times$ 20 mm), and continuously stirred by the magnet (the object dotted in red). The sample is illuminated from the direction illustrated by white arrow. The temperature sensor is circled red. d) Close up of the illuminated region, individual LC droplets are clearly visible due to emission. e) Microscope image of a lasing CLC droplet, showing: (i) 3D lasing from the central orange spot, (ii) the inner green lobes are Bragg WGM lasing modes, (iii) green light from the surface of the droplet presents lasing from the WGMs.

Optics EXPRESS

### 2.3. Lasing spectra measurements

The glass container containing the dispersion of CLC droplets was inserted into a temperature controlled chamber (Okolab) and temperature of the sample was controlled in the range from 22 °C to 55 °C. The temperature sensor was submerged in the sample near the spot where pump laser was focused, as shown in Fig.1(c). The temperature of the sample was slowly increased from room temperature until the sample reached the temperature of 42 °C. Above this temperature the Bragg lasing wavelength becomes so short that it falls outside of the filter transmission range.The cross-section of the beam focused by the telescope is ~2 $mm^2$, and the pump pulse energy used in the experiments is ~200 $\mu$J. The energy density at the beam waist therefore corresponds to ~10 $mJ/cm^2$, which is approximately 8-times above the lasing threshold, determined in the early 3D Bragg lasing experiments [12].

### 2.4. Results and discussion

In the experiments we observe a typical lasing spectrum, shown in Fig. 2(c) for mixture 1 at 27 °C. Three distinct lasing lines can be observed, which are attributed to different lasing modes. The small peak at 595 nm is attributed to the 3D Bragg lasing, i.e. the omnidirectional lasing mode, the lasing peaks at 569 nm and 556 nm are attributed to the Bragg WGM lasing from the inner cholesteric shells, whereas the peaks from 560-590 nm are attributed to the WGM lasing from the droplet's interface, as explained in the schematic Fig. 2(a). The cholesteric droplet with parallel surface anchoring at the surface can be considered as an onion-like photonic structure with alternating higher/lower value of the refractive index. The Bragg modes are radial modes corresponding to the radial photonic band gap, which results in omnidirectional 3D lasing from such a droplet. The onset of Bragg lasing is shown in the inset to Fig. 2(c), and is observed as a characteristic "knee" in the output intensity at the Bragg wavelength. The Bragg lasing can in principle occur at both edges of the photonic band gap, where the density of states is maximum. In reality, lasing in chiral nematic liquid crystals is usually observed only at one edge of the photonic band gap, because the optical gain is not equal on both edges. The optical gain in such a laser is due to fluorescent emission of the particular organic dye used in lasing experiments. The emission spectrum of a dye and also the transmission spectrum of our illumination optics is usually not symmetric with respect to the photonic band gap of the liquid crystal mixture, which means that lasing at one edge usually prevails over the lasing at the other edge of the band. In our experiments, lasing from the band edge at longer wavelengths was always dominant. We can therefore clearly recognize, which peak in the lasing spectrum corresponds to the Bragg lasing at the longer wavelength of the band edge at any given temperature. The Bragg lasing at 595 nm in Fig. 2(c) is small in intensity because it is not at the maximum gain wavelength region. By chance, this Bragg lasing peak at 36.7 °C coincides with the Bragg WGM peak at 27 °C, which might be a source of confusion. However, we can clearly monitor the shift of the Bragg lasing peak at different temperatures. With increasing temperature the 3D Bragg lasing peak moves into more optimal dye gain region and becomes much stronger.

In additional to the main Bragg lasing we also observe one or more lasing modes in the form of bright rings in the interior of the droplet. We term these modes "Bragg WGMs". These modes could originate from light circulating as WGMs within a given cholesteric shell, i.e. within one shell of the onion-like structure. A typical thickness of such a shell is one half of the helical period of the chiral nematic structure, which is around 200 nm. A second, more likely mechanism giving rise to Bragg WGMs are multiple Bragg reflections of light on the periodic structure so the light is circulating in the droplet [15]. Due to the Bragg condition, the reflection bandgap at shallower angle shifts to shorter wavelengths. If more Bragg WGMs are present in the droplet, the Bragg WGMs corresponding to outer rings always have shorter wavelength than those corresponding to inner rings, since the light is reflecting at shallower angles. The wavelength of the Bragg WGM lasing peaks has the same temperature dependence as the normal radial Bragg peak,

Optics EXPRESS

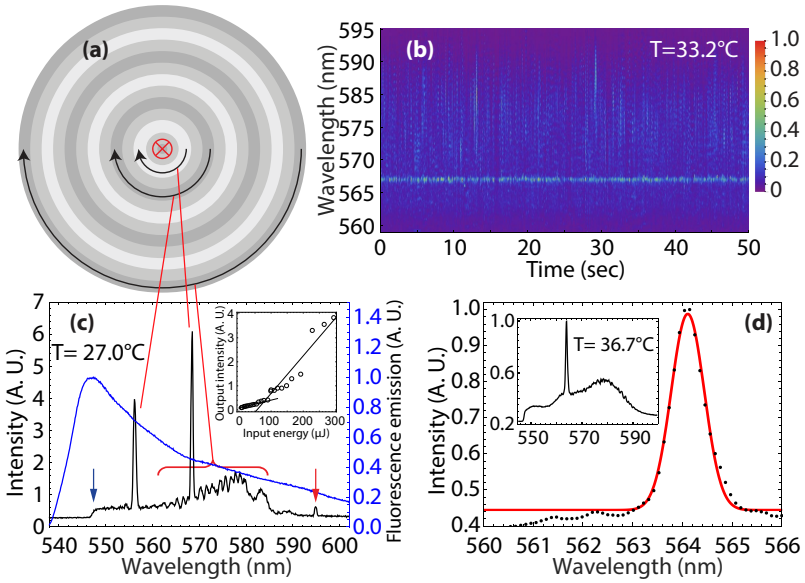


Fig. 2. a) Schematics of the origin of different kinds of lasing channels that appear in CLC droplets. The radial Bragg lasing is observed from the droplet center marked with red crossed circle. This gives rise to omnidirectional, 3D lasing. If the droplets are big enough, then the "inner shell", Bragg WGM lasing is observed, pictured with curved arrows near the center. The surface WGMs are sustained when refractive index of the carrier medium is much lower than both indices of the liquid crystal, pictured by the curved arrow along the surface. b) Time dependence of the 3D omnidirectional Bragg lasing from a number of different CLC droplets in glycerol. c) Typical spectrum, showing all three different kinds of lasing, which was obtained in sample 2 from a single droplet The fluorescence emission spectrum of the pyrromethene dye mixed in the LC mixture is also shown as blue curve, with the intensity scale on the right-hand side. The spectrum was measured under an optical microscope with the same optical filters as in the optical setup with the telescope. Black arrow indicates cut-off wavelength of the optical filters in the telescope system. Red arrow indicates the position of the Bragg lasing line. The inset shows the onset of Bragg lasing when the excitation pulses exceed ~100 $\mu$J energy per pulse. d) Close-up of the Bragg lasing line averaged from 200 accumulated spectra taken from sample 1. The red line is a Gaussian fit, from which temperature dependence was obtained. The inset shows the full spectrum.

further confirming that Bragg WGMs are dependent on the periodic structures and therefore most probably originate from Bragg reflections.

Radial Bragg and Bragg WGMs are not the only optical modes in the droplet. There is also ordinary WGM lasing present, where the light is circulating due to total internal reflection on the interface between the droplet and the outside medium. These modes are observable if the refractive index of the surrounding medium is considerably lower than the refractive indices of the cholesteric droplet. WGM lasing is highly dependent on the droplet size, therefore we do not employ WGM lasing for temperature measurements. If having a longer exposure time, so that multiple droplets pass excitation beam, the WGMs average out so that the individual peaks are not distinguished.

In experiments we usually observe one or more Bragg WGMs, which can be excited by positioning the excitation beam on that particular region of the droplet. An example is shown in Fig. 1(e). The green inner "lobe" represents the lasing from one Bragg WGMs, whereas the other green lobe at the edge of the droplet represents WGM lasing from droplet's interface. The orange

Optics EXPRESS

spot in the center of the droplet is the radial 3D Bragg lasing. By positioning the excitation beam to different parts of the droplet, different lasing lines become more prevalent.

After the lasing lines from a single CLC droplet were characterised with a microscope, we performed the measurements of the remote excitation and sensing of the light, emitted from CLC droplets, freely floating in the container, placed at a distance of ~ 1 m, as illustrated in the photograph of the set-up in Fig. 1(b). When a 10 ns excitation green pulse is sent through the telescope, it eventually excites fluorescent molecules in one or several CLC droplets that are by chance traversing the waist of the excitation beam at that moment. If the excitation pulse is strong enough, 3D lasing emission will be triggered from those CLC droplets, and some of the light will be emitted in the direction towards the telescope aperture. This light is the captured by the optics of the telescope and analysed by the spectrometer. In experiments the "flash-backs" of monochromatic light from individual CLC droplets can be clearly distinguished.

We have also measured the shape and dimensions of the "excitation volume", which is the volume within the dispersion of droplets, where the omnidirectional lasing is excited by the 250 $\mu$J, 532 nm light pulses sent from the telescope. Figure 3(a) shows the measured cross-section of the waist of the 532 nm excitation beam at approximately 1 m from the telescope front lens. The light intensity cross-section was measured from the image of the beam, taken by placing the image sensor of a camera directly into the excitation beam. The image of the excitation beam waist is presented in Fig. 3(b). The beam waist is approximately 1.5 mm wide, which is substantially larger than the theoretical diffraction-limited value of only 1.7 $\mu$m. This is due to using a multimode fiber to deliver the light from the laser to the optics as well because of optical aberrations of the optical system. We have also measured lasing intensity along-the-optical axis of the excitation in a separate sample with the same experimental set-up. In this case the sample was made of two glass plates separated by 120 $\mu$m spacers. The volume between the two plates was filled with glycerol dispersion of droplets made of the same CLC material. The diameter of the droplets was typically 70-80 $\mu$m and due to confinement the position of the droplets was fixed during the lasing experiment. The sample with droplets was positioned in the center of the beam waist and the lasing intensity from a single droplet was measured at different positions of the cell, which was moved along the optical axis. In this way we have obtained an indirect measure of the intensity profile of the excitation beam along the optical axis and in the vicinity of the focal point of the telescope set-up. The results are shown in Fig. 3(c). The "length" of the excitation volume along the optical axis is ~ 5 mm, which together with ~ 1.5 mm diameter corresponds to ~ 10 mm$^3$ excitation volume.

By accumulating multiple spectra, the WGM lasing from polydispersed droplets merged with the background fluorescence, because they all have different eigenfrequencies. On the other hand the Bragg lasing peak wavelength is only slightly different for different droplets and the

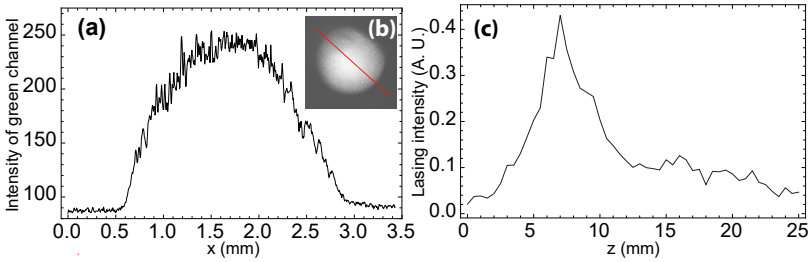


Fig. 3. The analysis of the excitation volume, from which the 3D omnidirectional lasing could be obtained: a) Beam profile at the focal point. b) Intensity of Bragg lasing at pump energy of 250 $\mu$J from a single droplet in glycerol as it was moved along the optical axis.

Optics EXPRESS

distribution of lasing wavelengths from poly-disperse sample of CLC droplets (in terms of the diameter of droplets) is rather sharp and is shown in Fig. 2(d). This distribution can be well fitted to the Gaussian curve, which in this case gives the lasing wavelength of 556.5 nm and the width of ~ 1 nm.

The spectra were measured while the sample was heated from 30 °C to 42 °C, and multiple spectra were accumulated for better contrast of the lasing signal at each selected temperature. After reaching 42 °C the sample was cooled down to 30 °C and the spectra was retaken and inspected for repeatability. We have found perfect repeatability of the measured emission wavelength for different temperature cycles.

The measured temperature dependence of the lasing spectra is presented in Fig. 4(a). The most dominant spectral line corresponds to the 3D omnidirectional Bragg lasing, whereas the lasing lines at shorter wavelengths correspond to Bragg WGMs. We have analysed in more detail the omnidirectional Bragg lasing peak, because we want to use this signal for remote, autonomous and omnidirectional measurement of the local temperature, sensed by the CLC droplet. The temperature dependence of the omnidirectional Bragg lasing peak was obtained from fitting a Gaussian curve to each Bragg lasing peak such as in Fig. 2(d). The resulting temperature dependence of the omnidirectional Bragg lasing is presented in Fig. 4(b). The integration time for individual spectrum at one temperature is 10 s, however the same measurement with somewhat lower accuracy could be made with just a few laser pulses which would take less than a second. We find that the temperature dependence of the omnidirectional lasing line is best described by the equation:

$$\lambda_{Bragg\ lasing} = \frac{A}{T + T_{\circ}}, \tag{1}$$

where the fitting parameters are $A = 1.06 \cdot 10^5(1 \pm 0.001)$ nm/°C and $T_{\circ} = 152(1 \pm 0.0016)$ °C for the sample 1, which was optimised for the temperature range around body temperature. It is quite clear from the slope of the temperature dependence of the 3D Bragg lasing line in Fig. 4(b) that the CLC droplets are very sensitive micro-thermometers. The sensitivity of the measurement is determined by the slope of the lasing line $\lambda(T)$, which is ~ 3 nm/K. The center of the Bragg

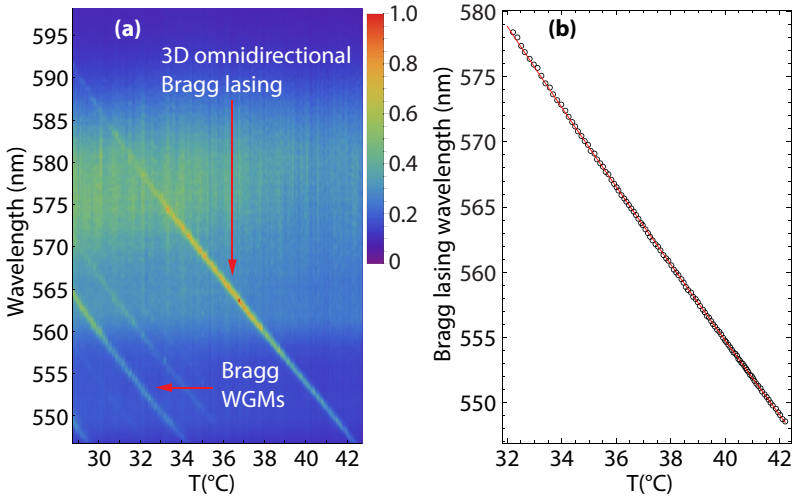


Fig. 4. a) Lasing spectra collected by the telescope at a distance of 1 meter from the sample. 150 spectra were measured at different temperatures, each spectra was accumulated from 200 laser pulses, captured at 20 Hz. b) Fit of the temperature dependence of Bragg lasing wavelength.

Optics EXPRESS

lasing line can be determined to better than 0.3 nm, which means that the temperature of the local environment of the CLC droplets can be measured to better than 0.1 K accuracy.

## 3. Conclusion

Our work clearly demonstrates proof-of-principle of using micrometer-sized CLC droplets for autonomous and remote sensing of temperature via Bragg omnidirectional excitation and lasing. The same technique could be applied to almost any responsive CLCs. For example, the CLCs have been made sensitive to pH [29], metal ions [30–32], amino acids [33], etc. This makes it feasible to design and develop novel CLC materials for the application in remote sensing of a variety of physical and chemical parameters. The only requirement is that the helical period of the chiral liquid crystal be sensitive-enough for that particular parameter or substance (and not to any other uncontrolled parameter). The method could be used in different liquid and even vapour environment and could be made chemically compatible with a particular environment by encapsulating the droplets in protective or active shells. We are convinced this opens many interesting applications in remote and autonomous optical sensing.

The method is also very robust with respect to photo-bleaching, which is the main technical obstacle for practical applications of dye-based liquid microlasers. Usually the small volume of the optical gain material prevents efficient regeneration of the dye molecules by flow or diffusion, which results in gradual decrease of the microlasers' output due to photo-bleaching of organic dye. When we perform the lasing experiment on a single liquid crystal droplet under the same illuminating conditions in an optical microscope, the droplet stops lasing after approximately 5 minutes of operation or 6.000 emitted pulses. However, in the experiments with remote excitation and detection we used the same sample for a couple of weeks without noticing any decrease of the intensity of lasing from droplets. The reason is that we have a huge number of microlasers, estimated to approximately 1 million of microlaser droplets in the measuring volume of 12 $cm^3$. We also know from the experiments that due to Brownian motion, each droplet is excited only once, while passing the excitation volume, which results in very low photo-bleaching. This makes our measuring method very robust in comparison to using a single droplet as a microlaser sensor.

The sensitivity and sensing distance of the method could be further improved by using diffraction limited optics. Currently we excite the lasing at a distance of up to 3 m. However, diffraction limited optics with the same diameter can focus laser light to the same spot size of 1.5 mm to a distance of 0.5 km. By increasing the power of the laser to a few mJ, we could increase the laser excitation to several kilometers. More problematic would be the back detection of lasing signal from CLC droplets, since the lasers emit in all the directions, and the signal decreases as a square of the distance. At the distance of 3 m we have very good signal to noise ration, so even with a 10-fold lower signal we would be able to determine accurately the position of the laser peak. Together with the increase of laser power this would extend the detection distance to at least 30 m. By using diffraction limited optics also the light collection efficiency could be increased, further extending the reach of the detection. Due to the lasing signal being highly localized in time within few nanoseconds and narrow in wavelength within 1 nm it is relatively insensitive to ambient light. The laser excitation is also periodic which enables to use lock-in detection to further increasing signal-to-noise ratio. Further improvements are possible in increasing the speed of measuring the temperature. Currently we are using the excitation pulsed laser with the repetition rate of 20 Hz and the temperature resolution of 0.1 K can be reached by accumulating 200 pulses, which takes 10 s of time. By increasing the repetition rate of the excitation laser ten fold, the temperature could easily be monitored in real time. This work could open up numerous application of remote and autonomous sensing in industrial, environmental and ambient research and monitoring.

Optics EXPRESS

## Funding

Slovenian Research Agency (ARRS) (P1-0099, L1-8135); H2020 Marie Skłodowska-Curie Actions (MSCA)(702715).